

energy [Eq. (7)]. We do not discount contributions from kinks and phonons but merely assert their small weight for \hat{S}_{cc} in contrast to the other spectral densities, as considered in Ref. 1.

To summarize, the present and our previous study¹ have revealed that all three fundamental normal modes of the sine-Gordon equation, the linear phonon mode, the nonlinear kink, antikink, and breather modes give rise to resonances in the thermalized sine-Gordon chain. In particular, although the breather is a well-documented solution to the continuous and deterministic problem,^{2,3,5,6} it has not previously been shown that these coherent anharmonic phonon effects persist in statistical mechanics or they have the strong response characteristic shown here. In view of the lack of any method providing reliable estimates of the spectral densities of such nonlinear systems, we hope that these results will stimulate theoretical work in this area. Moreover, our results suggest that the spectral density measured in the one-dimensional XY-like ferromagnetic CsNiF₃ in a parallel field should be interpreted in terms of breathers and magnons in contrast to current interpretation.¹⁰

^(a)Permanent address: Physics Department, Queen Mary College, Mile End Road, London, England.

¹T. Schneider and E. Stoll, Phys. Rev. Lett. **41**, 1429 (1978).

²M. J. Ablowitz, D. J. Kaup, A. C. Newell, and H. Segur, Phys. Rev. Lett. **30**, 1262 (1973).

³L. A. Takhtadzhyan and L. D. Faddeev, Theor. Mat. Fiz. **21**, 160 (1974).

⁴P. J. Caudrey, J. C. Eilbeck, and J. D. Gibbon, Nuovo Cimento B **25**, 447 (1975).

⁵R. F. Dashen, B. Hasslacher, and A. Neveu, Phys. Rev. D **11**, 3424 (1975).

⁶D. J. Kaup and A. C. Newell, Proc. Roy. Soc. London, Ser. A **361**, 413-446 (1978).

⁷T. Schneider and E. Stoll, Phys. Rev. B **17**, 1302 (1978).

⁸T. Schneider and E. Stoll, Phys. Rev. Lett. **31**, 1254 (1973).

⁹H. J. Mikeska, J. Phys. C **11**, L 29 (1978).

¹⁰M. Steiner and J. K. Kjems, in *Solitons and Condensed Matter Physics*, edited by A. R. Bishop and T. Schneider (Springer, Berlin and New York, 1978); J. K. Kjems and M. Steiner, Phys. Rev. Lett. **41**, 1137 (1978).

¹¹S. E. Trullinger, M. D. Miller, R. A. Guyer, A. R. Bishop, F. Palmer, and J. A. Krumhansl, Phys. Rev. Lett. **40**, 206, 1603(E) (1978).

¹²L. D. Landau and E. M. Lifschitz, *Physique Statistique* (Edition MIR, Moscow, 1967), p. 138.

Quark Structure Functions of Mesons and the Drell-Yan Process

Edmond L. Berger^(a) and Stanley J. Brodsky

Stanford Linear Accelerator Center, Stanford University, Stanford, California 94305

(Received 18 January 1979)

For massive-lepton pair production in meson-induced reactions, we use quantum chromodynamics perturbation theory to predict that the decay angular distribution in the pair rest frame will change from predominantly $1 + \cos^2\theta$ to $\sin^2\theta$ as the longitudinal-momentum fraction of the pair $x_F \rightarrow 1$. The two angular distributions are associated respectively with $(1-x)^2$ and $Q^{-2}(1-x)^0$ components of the valence-quark structure function of the meson.

The Drell-Yan process¹ $A+B \rightarrow l\bar{l}X$ measures the ability of colliding hadrons to reconfigure their momentum into the local production of a massive lepton pair with four-momentum Q^μ . As the edge of phase space is approached (i.e., $\tau = Q^2/s \rightarrow 1$ or $x_F = Q_L/Q_L^{\max} \rightarrow 1$), an annihilating quark q or antiquark \bar{q} in the subprocess $\bar{q}q \rightarrow \gamma^* \rightarrow l\bar{l}$ is taken far off-shell, and consequently the far-off-shell, short-distance internal dynamics of the hadronic wave function is probed. The Drell-Yan process can thus be used to determine the structure functions of hadrons not normally accessible in deep-inelastic scattering and to measure other important aspects of the dynamics

(e.g., spin properties) of the hadronic constituents at short distance.

In this Letter, we report an analysis of meson-induced massive-lepton pair production, $MB \rightarrow l^+l^-X$, in the context of perturbative quantum chromodynamics (QCD). We go beyond the usual treatments by including explicit effects associated with the meson bound state.² We assume that in the low-momentum-transfer domain, the meson wave function describes a $q\bar{q}$ bound state, and that at large momentum transfer, the momentum dependence of the meson wave function is controlled by the Bethe-Salpeter kernel—and thus by single-gluon exchange in the asymptotic-

freedom limit. This idea is sketched in Fig. 1. The same model³ yields the standard predictions^{3,4} for the power behavior of meson and baryon form factors at large Q^2 , and for baryon valence structure functions, all consistent with experiment. Our focus here is on the consequences of the QCD description of internal hadron dynamics; logarithmic corrections due to QCD radiative processes can be treated in the conventional manner.

The most striking testable consequences of this QCD picture for $MB \rightarrow l^+ l^- X$ are its predictions for the valence-quark structure function of the meson and for the polarization of the virtual photon $\gamma^* \rightarrow l^+ l^-$. The structure function has both a scaling⁵ $[(1-x)^2]$ and a nonscaling⁶ $[Q^{-2}(1-x)^0]$ component, with specified relative magnitude. Each is associated with a different angular distribution in the lepton-pair rest frame. For $Mq \rightarrow l^+ l^- X$, we obtain

$$d\sigma \propto (1-x)^2(1 + \cos^2\theta) + \frac{4}{9} \langle \langle k_T^2 \rangle \rangle / Q^2 \sin^2\theta. \quad (1)$$

Here x is the momentum fraction (light-cone variable) of the annihilating \bar{q} from the meson, $\langle k_T^2 \rangle$ is the average of the square of its transverse momentum, and $\cos\theta = \hat{p}_1 \cdot \hat{p}_\pi$ is defined in the lepton-pair rest frame. Identification of the nonscaling piece in the data can be made in several different ways: the x dependence of the cross section at fixed Q^2, s ; the angular (θ) dependence at fixed x, Q^2, s ; and the s dependence at fixed Q^2/s .

The dominant contribution to $\pi^- N \rightarrow \mu^+ \mu^- X$ at large Q^2 arises from the annihilation $\bar{u}u \rightarrow \gamma^* \rightarrow \mu^+ \mu^-$, where the antiquark \bar{u} comes from the π^- and the u from the nucleon. We concentrate on the kinematic region where only the \bar{u} is far off-shell (i.e., $x_F \rightarrow 1$). It is sufficient to treat the u quark as nearly free and on-shell. Thus, the incident nucleon structure is not indicated in the lowest-order diagrams shown in Fig. 1 for $\pi^- q \rightarrow \gamma^* q$. Both diagrams in Fig. 1 are required by gauge invariance, although in a physical (axial) gauge, the scaling contributions as $Q^2 \rightarrow \infty$ can be identified solely with Fig. 1(a). We partition the

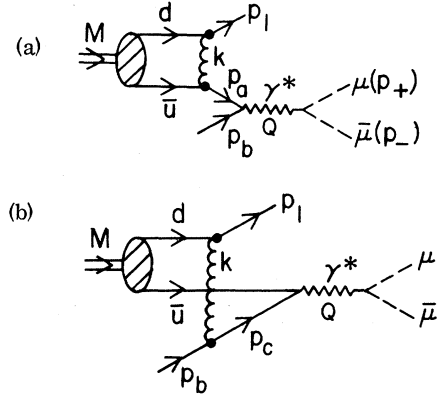


FIG. 1. Diagrams for $Mq \rightarrow q\gamma^*$, $\gamma^* \rightarrow \mu^+\mu^-$. Solid single lines represent quarks. Symbols p_1 , p_a , p_b , and p_c denote four-momenta of quarks, and k is the four-momentum of the gluon.

incident meson momentum p equally between the constituent q and \bar{q} ; this simplifying approximation can be discarded as it does not affect our conclusions.

The kinematics of the annihilating antiquark are specified with light-cone variables $x_a = (p_a^0 + p_a^3)/(p^0 + p^3)$, and k_{Ta} . Setting $p_1^2 = m^2$, where m denotes the bare quark mass, we use energy and momentum conservation to derive

$$p_a^2 = - \frac{\bar{k}_{Ta}^2 + x_a m^2 - x_a(1-x_a)m_\pi^2}{1-x_a}. \quad (2)$$

As $x_a \rightarrow 1$, p_a^2 becomes large and far spacelike. The squared four-momentum carried by the gluon in Fig. 1,

$$k^2 = (p_1 - \frac{1}{2}p)^2 = \frac{1}{2}(p_a^2 + m^2) - \frac{1}{4}m_\pi^2,$$

also becomes large as $x_a \rightarrow 1$. Therefore, invoking arguments based on asymptotic freedom, we suppose that in the range of x_a of interest to us, the single-gluon-exchange approximation shown in Fig. 1 will yield a good representation of the asymptotic large-momentum behavior of the Bethe-Salpeter kernel for the $q\bar{q}$ bound state.⁷

The invariant amplitude corresponding to Fig. 1 is

$$\mathfrak{M} \propto \bar{u}(p_+) \gamma_\mu v(p_-) \frac{1}{Q^2} \frac{\alpha_s(k^2)}{k^2} \psi_\pi(0) \sum_\lambda \bar{u}(p_1) \gamma_\alpha u_\lambda(\frac{1}{2}p) \bar{v}_\lambda(\frac{1}{2}p) \left[-\gamma^\alpha \frac{1}{\not{p}_a + m} \gamma^\mu + \gamma^\mu \frac{1}{\not{p}_c - m} \gamma^\alpha \right] u(p_b), \quad (3)$$

where $\sum_\lambda u_\lambda \bar{v}_\lambda = (\frac{1}{2}\not{p} + m)\gamma_5$ specifies that the $\bar{u}c$ bound state is a pseudoscalar.⁸ The factor $\psi_\pi(\vec{k}=0)$ in Eq. (3) represents an integration over the soft momenta in the pion wave function. We remark that our expression for the amplitude is precisely correct in the limit of zero binding energy for the meson. Note also that in our calculation the quark transverse momentum \bar{k}_T enters explicitly; it is not an arbitrarily assigned "intrinsic" or "primordial" \bar{k}_T associated with the $q\bar{q}$ binding in the wave function.

For simplicity in what follows, we set $m^2=0$ and $m_\pi^2=0$, and we restrict our attention to $\vec{k}_{Ta}^2 \ll Q^2$. Using the amplitude in Eq. (3), we compute an explicit expression for the cross section for $\pi^- N \rightarrow \mu^- \bar{\nu} X$. After integration over the azimuthal angle in the pair rest frame, we obtain

$$\frac{Q^2 d\sigma}{dQ^2 d^2Q_T dx_L d\cos\theta} \propto \int d^2k_{Ta} dx_a d^2k_{Tb} dx_b G_{q/N}(x_b, \vec{k}_{Tb}) \frac{\psi_\pi^2(0)}{k_{Ta}^4} \left[(1-x_a)^2 (1+\cos^2\theta) + \frac{4}{9} \frac{k_{Ta}^2}{Q^2} \sin^2\theta \right] \times \delta^2(\vec{Q}_T - \vec{k}_{Ta} - \vec{k}_{Tb}) \delta(x_L - x_a - x_b) \delta(Q^2 - x_a x_b S). \quad (4)$$

Here $G_{q/N}$ is the quark structure function of the nucleon. We have discarded contributions which are of order $Q^{-2} k_T^2 (1-x_a)$ and $Q^{-4} k_T^4 (1-x_a)^{-1}$ in the square brackets of Eq. (4).⁹ The contributions from sea quarks and antiquarks in the meson and nucleon are also ignored in Eq. (4).

In the Bjorken scaling limit, $Q^2 \rightarrow \infty$, at fixed x_a , the valence-quark structure function can be extracted from Eq. (4):

$$G_{\bar{q}/\pi}(x) = \int d^2k_T G_{\bar{q}/\pi}(x, \vec{k}_T) \propto (1-x)^2. \quad (5)$$

The corresponding \vec{k}_T falloff produces pairs with a Q_T^{-4} distribution² (for $k_{Ta}^2 \ll Q^2$).

We observe the following additional features of Eq. (4): (i) We can identify a nonscaling contribution to the structure function. After averaging over $\cos\theta$, we obtain

$$G_{\bar{q}/\pi} \sim (1-x)^2 + \frac{2}{9} \langle k_T^2 \rangle / Q^2. \quad (6)$$

The nonscaling contribution is independent of x and will dominate the scaling contribution at fixed $Q^2(1-x)$ as $Q^2 \rightarrow \infty$. In our model the relative magnitude of the scaling and nonscaling terms is fixed.⁹ When the nonscaling term dominates in Eq. (4), the mean $\langle k_{Ta}^2 \rangle$ is of order $Q^2/\ln Q^2$.

(ii) The nonscaling contribution corresponds to a longitudinal structure function and provides a $\sin^2\theta$ angular distribution in the lepton-pair rest frame, in contrast to the conventional expectation of $1+\cos^2\theta$. At fixed Q^2 , the $\sin^2\theta$ term dominates in the cross section as $x_F \rightarrow 1$. The usual rule that annihilating spin- $\frac{1}{2}$ quarks produce transversely polarized photons is modified when off-shell constituents are involved. In our case, the \bar{q} is kinematically far off shell since, as $x_F \rightarrow 1$, all of the momentum of the recoil spectator quark must be transferred to the annihilation subprocess. In this situation the spin of the incident meson influences the final angular distribution. In a different language, the bound-state effect can be identified with a "high-twist" subprocess, since more than the minimum number of elementary fields is required.

In the range $4.0 \leq M = (Q^2)^{1/2} \leq 8.5$ GeV, an effective pion structure function has been extracted by Newman *et al.*¹⁰ from their data on $\pi^- N \rightarrow \mu^+ \bar{\nu} X$

at 225 GeV/c. They report that $x G_\pi^{\text{expt}}(x) \simeq 0.5(1-x)^{1.01 \pm 0.05}$ for $x > 0.3$. For similar values of Q^2 , our structure function in Eq. (6) can mimic the observed $(1-x)^1$ behavior if we choose $\langle k_T^2 \rangle \simeq 1$ GeV². This value of $\langle k_T^2 \rangle$ is consistent with measured¹⁰ values of $\langle Q_T^2 \rangle = \langle (\vec{k}_{Ta} + \vec{k}_{Tb})^2 \rangle$. We remark parenthetically that the parameter $\langle k_T^2 \rangle$ in our formulas is a function of Q^2 and x and effectively includes the mass terms which were dropped when we set m^2 and $m_\pi^2=0$. Shown in Fig. 2(a) is a comparison of our structure function, Eq. (6), for different values of Q^2 , with the form $G_\pi^{\text{expt}}(x)$ deduced from the data, assuming Q^2 independence. We urge that the analysis of the data be repeated with Eq. (6).

In Fig. 2(b) we present our prediction for the polarization parameter α in the expression $d\sigma/d\cos\theta = 1 + \alpha \cos^2\theta$. In our model, $\alpha = (1-r)/(1+r)$, with

$$r = \frac{4}{9} \langle k_{Ta}^2 \rangle / Q^2 (1-x_a)^2. \quad (7)$$

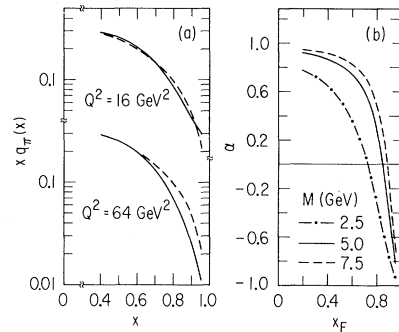


FIG. 2. (a) The quantity $x q_\pi(x)$ as a function of x for two values of Q^2 near the top and bottom of the range explored experimentally. Here we set $x q_\pi(x) = 2x G_{\bar{q}/\pi}$ with $G_{\bar{q}/\pi}$ provided in Eq. (6), and $\langle k_T^2 \rangle = 1$ GeV². The factor 2 is chosen to reproduce approximately the normalization of the experimentally deduced effective $x q_\pi(x)$ near $x=0.5$. For comparison, we plot as a dashed curve the experimental form (Ref. 10) $0.5(1-x)^{1.01}$. The computations in this paper are applicable only for $x > 0.5$. (b) Predicted value of α as a function of x_F for different values of M [$= (Q^2)^{1/2}$] at $p_{\text{lab}} = 225$ GeV/c, with $\langle k_T^2 \rangle = 1$ GeV².

Our predictions are presented as a function $x_F = (x_a - \tau/x_a)/(1 - \tau)$. The angle θ is referred to the t -channel (or Gottfried-Jackson) system of axes: $\cos\theta = \hat{p}_\mu \cdot \hat{p}_\pi$. Observed values of α are reported¹⁰ only for data averaged over all x_F , and, as we expect in this case, $\alpha \approx 1$ for $4 < M < 8.5$ GeV.

The experimental observation of an effective $(1-x)^1$ behavior of the quark structure function of the pion is incompatible with general crossing arguments for Born diagrams which mandate only even powers of $1-x$ as $x \rightarrow 1$ when a fermion is extracted from a meson.¹¹ The linear behavior $(1-x)$ would be expected, or *spinless* quarks. On the other hand, the spin- $\frac{1}{2}$ nature of the constituents seems well established by the observation in the same experiment of a decay angular distribution of $1 + \alpha \cos^2\theta$ with $\alpha \approx 1$. Our analysis provides a resolution of this apparent paradox. We suggest that the observed $(1-x)^1$ behavior is an approximation to our Eq. (6), in which only even powers of $1-x$ appear. The critical test of this assertion is the identification of the predicted $\sin^2\theta$ behavior of the decay angular distribution at large x_F .

Observation of our predicted $\sin^2\theta$ nonscaling term in the data would reinforce the applicability of the Drell-Yan model with spin- $\frac{1}{2}$ quarks and verify that structure functions can be understood in some detail in a QCD framework. Failure would mean that there is no fundamental explanation for the observed power behavior of structure functions. The nonscaling and angular-dependent effects we derive are in addition to, but much stronger than, analogous effects provided by QCD gluonic radiative corrections; in particular, our prediction for the angular distribution applies at small Q_T , where gluonic radiative corrections do not upset the conventional $1 + \cos^2\theta$ expectation.¹² The form we derive for the structure function in Eq. (6) should apply universally; for example, an analogous structure function should also be observed in meson-induced large- p_T hadronic processes.¹³

In baryon- (or antibaryon-) induced reactions, $BB \rightarrow l\bar{l}X$, the $1 + \cos^2\theta$ behavior characteristic of spin- $\frac{1}{2}$ systems is maintained as $x \rightarrow 1$. However, nonscaling longitudinal contributions arise near $x = \frac{2}{3}$ if we take into account the subprocess $(qq) + \bar{q} \rightarrow q + \gamma^*$ with a bosonic diquark system.¹⁴ These effects may be related to the anomalous values of σ_L/σ_T observed in deep-inelastic electron scattering¹⁵ at moderate values of Q^2 .

We thank R. Blankenbecler for helpful conver-

sations.

^(a)Permanent address: High Energy Physics Division, Argonne National Laboratory, Argonne, Ill. 60439.

¹S. D. Drell and T.-M. Yan, Phys. Rev. Lett. **25**, 316, 902(E) (1970). For a recent review see E. L. Berger, in *New Results in High Energy Physics*, AIP Conference Proceedings No. 45, edited by R. S. Panvini and S. E. Csorna (American Institute of Physics, New York, 1978).

²M. Duong-van, K. V. Vasavada, and R. Blankenbecler, Phys. Rev. D **16**, 1389 (1977); C. Debeau and D. Silverman, SLAC Report No. SLAC-PUB-2187, 1978 (unpublished).

³S. J. Brodsky and G. R. Farrar, Phys. Rev. Lett. **31**, 1153 (1973), and Phys. Rev. D **11**, 1309 (1975).

⁴V. A. Matveev, R. M. Muradyan, and A. N. Tavkhelidze, Lett. Nuovo Cimento **7**, 719 (1973).

⁵Z. F. Ezawa, Nuovo Cimento **23A**, 271 (1974).

⁶G. R. Farrar and D. R. Jackson, Phys. Rev. Lett. **35**, 1416 (1975). Our results are analogous to those for $e^+e^- \rightarrow \pi X$ derived by Farrar and Jackson. However, in the Drell-Yan process, the dominance of the longitudinal term at large x cannot be attributed to exclusive channels. See also A. I. Vainshtain and V. I. Zakharov, Phys. Lett. **72B**, 368 (1978).

⁷See, e.g., T. Appelquist and E. Poggio, Phys. Rev. D **10**, 3280 (1974), and Ref. 3. A detailed discussion will be given by S. J. Brodsky and P. Lepage, to be published. For a similar problem in quantum electrodynamics, see W. Caswell and P. Lepage, Phys. Rev. A **18**, 810 (1978).

⁸Our results also hold when the quark spins are uncorrelated.

⁹Our results are accurate in two $Q^2 \rightarrow \infty$ limits: (a) the fixed- x_a Bjorken limit, and (b) the fixed- $W^2 = (1-x)Q^2/x$ limit, with $W^2 \gg k_T^2$. The neglected terms in Eq. (4) must be retained at modest Q^2 for x very close to 1 (> 0.95).

¹⁰C. B. Newman *et al.*, Phys. Rev. Lett. **42**, 951 (1979) (this issue), and private communications.

¹¹S. D. Drell, D. J. Levy, and T.-M. Yan, Phys. Rev. D **1**, 1617 (1970). For a discussion of non-Born diagrams, see P. V. Landshoff and J. C. Polkinghorne, Phys. Rev. D **6**, 3708 (1972).

¹²K. Kajantie, J. Linfors, and R. Raitio, Phys. Lett. **74B**, 384 (1978); E. L. Berger, J. T. Donohue, and S. Wolfram, Phys. Rev. D **17**, 858 (1978); Berger, Ref. 1.

¹³A measurement of the quark structure function of the pion as seen in pion-induced hadronic jets is reported by M. Dris *et al.*, Pennsylvania University Reports No. UPR-39E (Rev.) and No. UPR-55E, 1978 (unpublished).

¹⁴In deep-inelastic processes, $\gamma^* + (qq)$ subprocesses have been considered by I. A. Schmidt, Ph.D. thesis, Stanford University SLAC Report No. 203, 1977 (unpublished); I. A. Schmidt and R. Blankenbecler, Phys. Rev. D **16**, 1318 (1977).

¹⁵E. M. Riordan *et al.*, Phys. Rev. Lett. **33**, 561 (1974); R. E. Taylor, in *Proceedings of the International Symposium on Lepton and Photon Interactions at High En-*

ergies, Stanford, California, 1975, edited by W. T. Kirk (SLAC, Stanford, Calif., 1975); W. B. Atwood, SLAC Report No. 185, 1975 (unpublished).

Production of Muon Pairs by 225-GeV/c π^\pm , K^\pm , p^\pm Beams on Nuclear Targets

K. J. Anderson, R. N. Coleman,^(a) G. E. Hogan, K. P. Karhi, K. T. McDonald, C. B. Newman, J. E. Pilcher, E. I. Rosenberg, G. H. Sanders,^(b) A. J. S. Smith, and J. J. Thaler
Enrico Fermi Institute, University of Chicago, Chicago, Illinois 60637, and University of Illinois, Urbana, Illinois 61801, and Joseph Henry Laboratories, Princeton University, Princeton, New Jersey 08540
 (Received 22 January 1979)

Results are presented from a large-acceptance experiment in which muon-pair production was observed in the mass range 2 to 11 GeV/c². Data were taken with π^\pm , K^\pm , and p^\pm beams at 225 GeV/c on carbon, copper, and tungsten targets. Differential cross sections and the production dependence on pair mass, x_F , p_T , incident-particle type, and target nucleus are discussed.

Lepton-pair production in hadron interactions has been a particularly fruitful area for testing current ideas on hadronic structure. In this Letter we report the most recent of a series of measurements on μ -pair production. The data have more than a factor of 50 greater sensitivity than our previous measurements¹ and explore several features of the production which have not been studied before.

The measurements were carried out with the Chicago cyclotron magnet spectrometer in the Muon Laboratory at Fermilab. The basic configuration of the spectrometer is discussed in our previous work.¹ The major modifications for this experiment consisted of, (1) installation of larger multiwire proportional chambers upstream of the cyclotron magnet to increase acceptance at low Feynman x (x_F) and high pair mass, (2) addition of a second large hodoscope array downstream of the magnet, and (3) addition of mass-threshold logic to the trigger to permit the use of higher-intensity incident beams. Details of the trigger, mass-threshold logic, and the spectrometer are presented elsewhere.² Improvements in the beam-line configuration resulted in an order-of-magnitude increase in available beam intensities.

An unseparated positive or negative beam of 225-GeV/c hadrons (π^\pm, K^\pm, p^\pm) was focused to a 2-cm \times 3-cm spot at the experimental target. Four threshold gas Cherenkov counters were placed in the beam to identify the particle type. For negative running, all counters were set just below \bar{p} threshold. For positive beams, two coun-

ters were set below K threshold and two were set below proton threshold. The pion component of the positive beam was enhanced at the expense of total transmission, by placing a polyethylene absorber in the beam about 300 m upstream of the spectrometer. With this absorber pions constituted 28% of the positive flux. The resulting positive beam intensity was kept below 10⁷/sec to allow π - K - p separation. Negative intensities of up to 2 \times 10⁷/sec were obtained.

Carbon, copper, and tungsten targets, each 1 absorption length thick, were used. The carbon target was divided into three segments of equal thickness, separated by scintillation counters. The scintillator pulse heights were used to localize the beam interaction point and hence to test for thick-target effects. Production of μ pairs by secondary particle interactions in the target would appear as an excess of counts at low Feynman x ($x_F = P_L^*/P_{\max}^*$) for the events originating in the downstream target segment. A comparison of x_F distribution of 10 000 J/ψ events originating in the upstream and downstream target segments reveals no evidence of secondary interactions.

For reasons described in the following paper,³ a carbon target was used to measure μ -pair production cross sections from π^+ and π^- beams. Special care was taken to maintain similar operating conditions for the two beam polarities. Following this phase of running, Cu and W targets were used with the highest available negative-beam rates.

The event reconstruction is very similar to that of our previous experiment which has already